January 1, 1994

Comparison between calculatedand observed F-region density profiles at Jicamarca, Peru

A. J. Preble
D. N. Anderson
Bela G. Fejer, *Utah State University*
P. H. Doherty

Radio Science, Volume 29, Number 4, Pages 857–866, July–August 1994

Comparison between calculated and observed *F* region electron density profiles at Jicamarca, Peru

Amanda J. Preble,[1] David N. Anderson,[2] Bela G. Fejer,[3] and Patricia H. Doherty[4]

Abstract. Electron density profiles and isodensity contours derived from Jicamarca incoherent scatter radar observations in Peru for October 1–2, 1970, are compared in detail with results from the Phillips Laboratory global theoretical ionospheric model. This model solves the ion continuity equation for O^+ concentration through production, loss, and transport of ionization. The primary factor controlling the peak plasma density at Jicamarca is the vertical **E** × **B** drift, which drives the ionization upward during the day and downward at night. When we use the measured drift in the model, we achieve excellent results with the measured electron density profiles. We illustrate the sensitivity of the low-latitude plasma density calculations to changes in the vertical **E** × **B** drift and changes in the neutral winds. We also compare the calculated profiles and peak parameters with an empirical model, the International Reference Ionosphere (IRI). We illustrate several limitations associated with the IRI that contribute to its limited capability at the magnetic equator.

Introduction

The equatorial F_2 region is a complex and dynamic region of the ionosphere where a variety of processes affect the plasma concentration. The plasma concentration is determined primarily by solar ionization during the day, but as altitude increases, transport processes such as ambipolar diffusion, neutral wind effects, and electrodynamic drifts play an increasingly important role in addition to local production and loss processes in determining F_2 region plasma densities [e.g., *Kelley*, 1989]. It has been shown that the height and shape of the F_2 layer at the magnetic equator is strongly dependent on the vertical **E** × **B** drift mechanism [*Hanson and Moffett*, 1966; *Sterling et al.*, 1969; *Anderson*, 1973a, b]. Early studies that used both drift and density measurements from Jicamarca include the computation of the daytime *F* region ionization distribution during periods of a solar eclipse [*Sterling et al.*, 1972] and of a great magnetic storm [*Woodman et al.*, 1972]. Later, *Bilitza* [1985] compared the *F* region peak parameters measured at Jicamarca with the results from the IRI, and *Anderson et al.* [1987] compared a single profile from Jicamarca with the semiempirical low-latitude ionospheric model (SLIM) and the *Chiu* [1975] models. To date, with the exception of a recent paper by *Bailey et al.* [1993], there has not been a detailed comparison of calculated and observed electron density profiles over Jicamarca when the measured electron plasma drifts were used as a model input.

Several approaches have been used to model the equatorial ionosphere and an excellent review of low-latitude ionospheric modeling is presented by *Stening* [1992]. The "climatological" approach uses an extensive amount of data and averages them by solar cycle and season or month. The *Chiu* [1975] model and the IRI [*Bilitza*, 1990] are examples of these models. The advantage to the climatological approach is its computational speed, and, in the case of the IRI, its global coverage. However, the trade-off is that temporal fluctuations in the ionosphere tend to be smoothed over in the averaging process. In the physical or theoretical approach the coupled continuity and momentum equations are solved for the electron/ion concentrations. As such, all the physical processes that determine the plasma concentrations may be included in the calculations

[1] Flight Test Branch, Phillips Laboratory, Kirtland Air Force Base, New Mexico.

[2] Ionospheric Effects Branch, Phillips Laboratory, Hanscom Air Force Base, Massachusetts.

[3] Center for Atmospheric Space Sciences, Utah State University, Logan.

[4] Institute for Space Research, Boston College, Newton, Massachusetts.

Paper number 94RS00825.
0048-6604/94/94RS-00825$08.00

and the day-to-day fluctuations are not averaged out. These theoretical models have the advantage that they can be readily coupled to other regional theoretical ionospheric, thermospheric, and magnetospheric models. This is particularly important at low latitudes where strong electrodynamic coupling exists between the ionospheric plasma and neutral winds via the F region dynamo process [*Stening*, 1981; *Fejer*, 1991; *Crain et al.*, 1993a, b]. The theoretical models may also be used to study the sensitivity of ionospheric parameters to changes in various input parameters such as neutral atmospheric constituents, solar production rates, and transport mechanisms [*Anderson*, 1973a, b; *Klobuchar et al.*, 1991]. To the degree that we can realistically specify the input parameters, current state-of-the-art theoretical ionospheric models can reliably model the plasma densities.

The purpose of this study is twofold. First, it is to compare theoretically calculated electron density profiles at the magnetic equator with the observed Jicamarca profiles, incorporating into the calculations observed drifts during an equinoctial period of quiet magnetic and moderate solar activity. We also examine the effect of the vertical drift and neutral winds on the electron density profiles. Previous theoretical modeling efforts using the Phillips Laboratory model and Jicamarca drifts have concentrated on investigations of the formation and decay of the equatorial anomaly [e.g., *Klobuchar et al.*, 1991]. The second purpose of the study is to compare the calculated profiles with the climatological-based IRI [*Bilitza*, 1990] to determine how well ionospheric parameters such as h_mF_2, N_mF_2 and profile shapes compare. With the exception of the 1400 LT comparison presented by *Anderson et al.* [1987], no similar detailed validation has been carried out over Jicamarca.

Observations and Theoretical Model

Experimental Data

The Jicamarca incoherent scatter radar (11.95°S, 76.87°W geographic, magnetic dip 2°N) has been used extensively for ionospheric studies since 1968 [*Farley*, 1991]. Details about the radar, its operations, and methods of observations and data analysis may be found in several publications (e.g., *McClure et al.* [1970] and *Farley* [1991] for operations; *Woodman and Hagfors* [1969] for details on the vertical drift technique). An extensive review of the vertical drifts observed by the Jicamarca radar may be found in work by *Fejer* [1991] and *Fejer et al.* [1991].

Figure 1 shows the plasma density contours in a logarithmic scale, measured on October 1–2, 1970, over Jicamarca. The height resolution of the electron density and plasma drift measurements was about 20–30 km and the integration time was about 10–15 min. The estimated error in density for these contours is less than 5% for densities greater than 10^4 electrons/cm^3 [*McClure et al.*, 1970]. The dashed line represents the peak layer height (h_mF_2) and traces the diurnal variations of the peak electron concentration (N_mF_2). The hatched area around sunset denotes the occurrence of equatorial spread-F, which masks the incoherent scatter signal [*McClure et al.*, 1970]. These data correspond to quiet time, moderate solar conditions with a daily $F_{10.7}$ cm flux of 128.7 units and a 90 day average of 146 units. Observed peak densities range from 4.0×10^5 cm^{-3} prior to sunrise to values around 1.2×10^6 during the day. The peak layer heights vary from approximately 270 to 560 km with the largest heights associated with the evening prereversal enhancement in the vertical $\mathbf{E} \times \mathbf{B}$ drift.

The observed vertical plasma drift velocity (in meters per second) is presented at the bottom of Figure 1. The positive values indicate upward drifts (driven by the eastward electric field). The strong upward and downward value of the drift, especially around sunset, is well known. The vertical drifts for this day fall within the variability of the solar moderate, equinoctial drifts as presented by *Fejer et al.* [1991]. In the following paragraphs we describe briefly our ionospheric model and then proceed to compare the experimental and numerical results.

Model Description

The Phillips Lab low-latitude ionospheric model solves the O^+ continuity equation as a function of altitude, latitude and local time to give plasma density profiles from 100 to 1600 km every 2° for every half hour local time. We feel that this single species model is sufficient for this study since we are considering moderate solar activity when light ions (H^+ and He^+) are important only above approximately 1000 km at the equator. In addition, we are only concerned with the radar measurements at F_2 region heights where molecular ions do not play an important role.

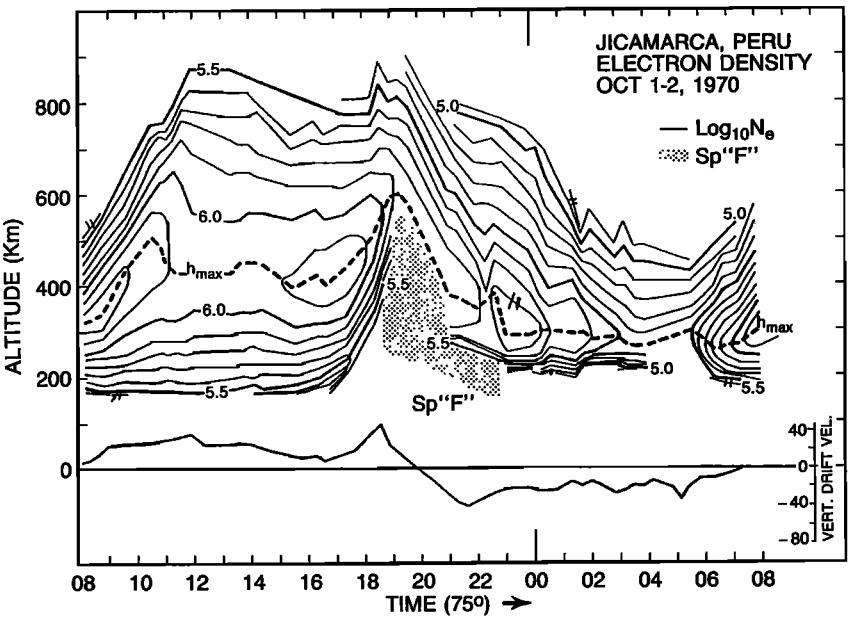

Figure 1. Measurements from 0800 on October 1 to 0800 on October 2, 1970, over Jicamarca, Peru. The contours of electron density (log 10) are presented as a function of altitude and local time in the top portion, the measured vertical drift (in meters per second) as a function of local time is presented in the bottom portion.

The model solves the plasma continuity equation

$$\frac{\partial N_i}{\partial t} + \mathbf{V}_{i\perp} \cdot \nabla N_i = P_i - L_i - \nabla(N_i \mathbf{V}_{i\parallel}) - N_i \nabla \cdot \mathbf{V}_{i\perp} \tag{1}$$

where P_i and L_i are the ion production and loss rates per unit volume, and $\mathbf{V}_{i\perp}$ and $\mathbf{V}_{i\parallel}$ denote the perpendicular and parallel components of the ion velocity. A number of authors have described the transformations necessary to numerically solve this second-order partial differential equation [*Hanson and Moffett*, 1966; *Anderson*, 1973a; *Moffett*, 1979]. We do not discuss it here.

In order to solve (1) the following input parameters as a function of altitude, location, time, solar activity, and magnetic activity are used in our low-latitude model:

1. The neutral atmospheric densities of N_2, O_2, and O, and the neutral temperature are obtained from the mass spectrometer/incoherent scatter neutral atmosphere model (MSIS-86) [*Hedin*, 1987].

2. The production and loss rates of O^+ are given by *Klobuchar et al.* [1991].

3. The ion and electron temperatures are based on the analytic functions of *Strobel and McElroy* [1970] and the solar EUV fluxes were derived from the algorithms of *Hinteregger et al.* [1981].

4. The horizontal neutral wind is obtained from the empirical wind model (HWM-87) of *Hedin et al.* [1988]. The differences between HWM-87 and HWM-90 [*Hedin et al.*, 1991] did not affect this study.

5. Finally, for the vertical **E** × **B** drift inputs we have used the vertical drift velocities shown in Figure 1, as well as a new 2-month averaged drift model (B. G. Fejer, personal communication, 1992) based on observations from Jicamarca on geomagnetically quiet, solar moderate ($F_{10.7}$ cm flux 100–170 units), equinoctial days which were centered around October 1. In addition, we compare the diurnal variation of N_mF_2 and h_mF_2 when the vertical drift is set to zero and when it is a factor of 1.5 times the measured value.

Comparison Between Observed and Calculated Profiles

E × B Drift Effects

The contour plot obtained using the measured drifts in GTIM (Figure 2) provides a summary of the

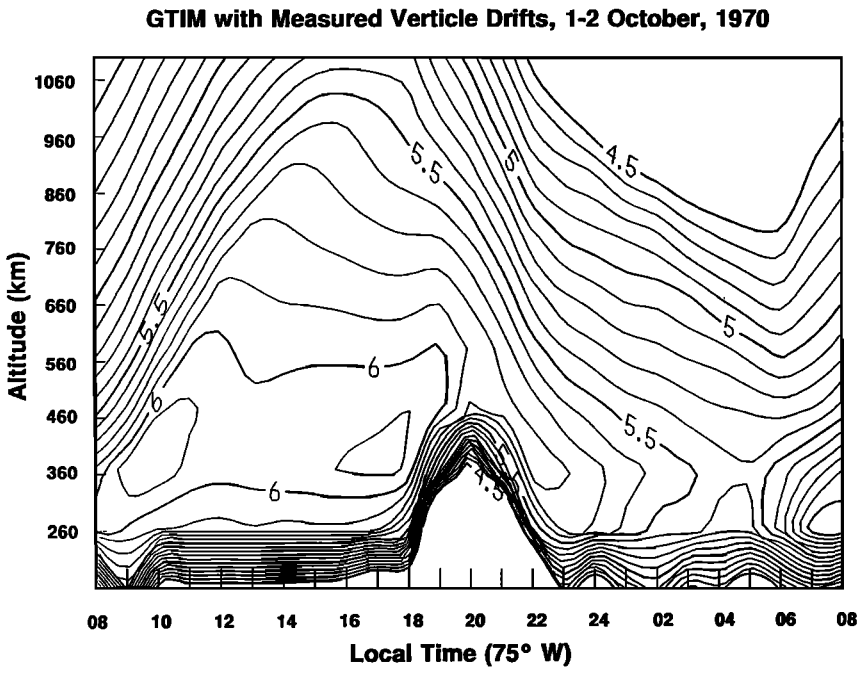

Figure 2. Modeled isodensity contours derived from the Phillips Laboratory ionospheric model calculations using the measured vertical drift as input.

capabilities of the model. The increased ionization and layer height increase in the morning sector, the noon bite-out that results from the rising layer, and the afternoon and postsunset increase in ionization are all represented by the model. The agreement between measured and model results is even more impressive around sunset where the enhancement in upward drift after 1800 LT raises the F layer peak to a height of 500 km at 2000 LT. There is a corresponding peak plasma density decrease from 1.4×10^6 cm^{-3} and 1.36×10^6 cm^{-3} to 7.08×10^5 cm^{-3} and 8.08×10^5 cm^{-3} for experimental and modeled results, respectively. Subsequent to the postsunset descent of the layer, after 2200 LT, h_mF_2 drops to 250 and 300 km and remains at these respective altitudes for the remainder of the night. The peak density decreases to a minimum value of 3.16×10^5 cm^{-3} and 3.26×10^5 cm^{-3} for experimental and modeled results, respectively. When the vertical drift is set to zero in the model, the contours we generate are almost horizontal because the layer is neither raised nor lowered. We increased the observed drift by a factor of 1.5 and found that there was little change in the daytime contoured results, but the evening prereversal enhancement shows an increase of 100 km as compared with the measured-drift results. This, in turn, modifies the nighttime density.

Figure 3 illustrates the peak height and maximum electron density and the model results calculated using as inputs zero vertical drift, the measured drifts, and the 2-month average drift. In each case the heavy solid line is used to represent the observed data. As expected, the agreement is best when the measured vertical drift is used to calculate the peak layer height (Figure 3a) and plasma density (Figure 3b). The 2-month average drifts also give good results. Between 1000 and 1200 LT, the higher h_mF_2 for the observed drift results are attributed to the very broad peak associated with the profile at this particular time. As a result, we have found that the model may overestimate h_mF_2 under conditions of strong upward drift during the day. The prereversal enhancement seen in the data and actual-drift model profiles at 2000 LT is almost 40 km greater than the h_mF_2 value from the average-drift model. Since the vertical drift is the primary force in determining the peak layer height in the equatorial regions, there is no surprise that with no vertical drift there is virtually no variation in h_mF_2. In fact, the zero-drift layer height never gets far above 400 km. The zero-drift layer increases from 0800 to 0600

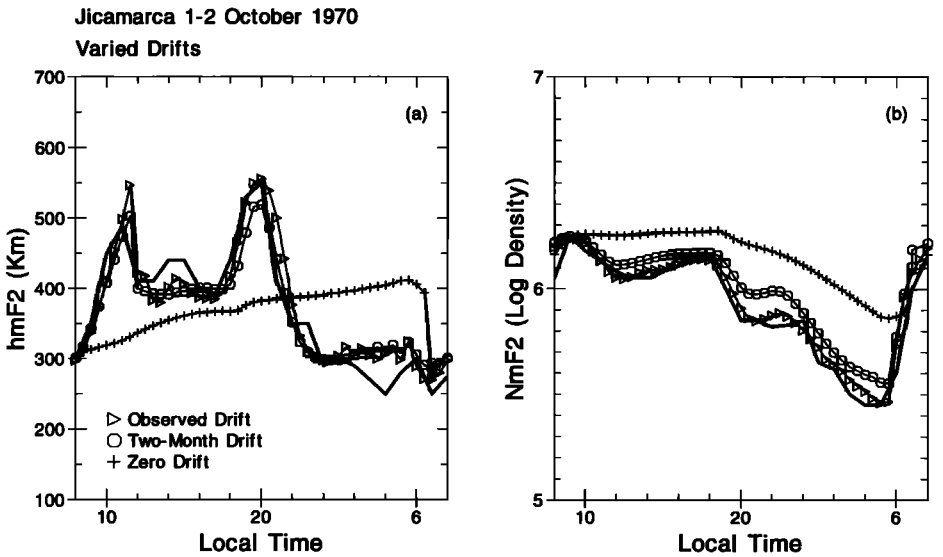

Figure 3. Comparisons of measured and calculated F region (a) peak layer height and (b) peak electron density for October 1–2. Measured h_mF_2 and N_mF_2 are shown as the heavy, solid line.

the next morning where the layer height drops off sharply.

The effects of the variation in **E** × **B** drift on the peak density are very apparent in Figure 3b. The agreement between the calculated and observed results again is excellent when the measured drifts are used. The average-drift results show a higher N_mF_2 than the data from midday throughout the early morning hours. We explain this difference by referring to the midday change in h_mF_2 in Figure 3a which shows a 50 km increase in h_mF_2 between 1300 and 1600 LT. The model with the measured drift is able to reproduce this change, but the average-drift results show a constant h_mF_2 of 400 km from 1100 to 1800 LT. Because the average-drift layer is not raised as much as the observed layer, there is less of a noon bite-out in ionization. Consequently, the layer density is higher when it undergoes prereversal enhancement and a denser layer remains after sunset. It can also be seen that in the average drift case the evening prereversal enhancement does not raise the layer as high as the actual data. This effect on the density is seen in the less sharp postsunset decrease in N_mF_2 in the average-drift layer when compared with the data layer and the actual-drift layer.

In the zero-drift case we showed that there was no transport mechanism to change the height of the layer. Therefore ionization is not transported away from the magnetic equator, resulting in higher peak densities seen in Figure 3b. At night the denser zero-drift layer decays solely from the effects of the chemical recombination.

In Figure 4 we illustrate the vertical profiles for 1200 and 1900 LT obtained when we increased the observed drift by a factor by 1.5 in the model. In the increased-drift case the noontime layer is not raised any higher than the original calculated results, h_mF_2 is actually at 420 km instead of 450 km. However, the corresponding profile is broader and the topside layer (above 600 km) is around 100 km higher than both the data and the observed-drift layer. The agreement between measured and calculated layer thickness and topside and bottomside profiles is excellent for the observed-drift profile.

The drift sensitivity is clearly illustrated by the profiles at 1900 LT. This was just after the peak evening prereversal enhancement of the upward drift where the increased drift substantially raised the layer height. At 1900 LT the peak heights were 550 km for the measured data, 520 km for the model results with observed drifts, and 600 km for the increased-drift calculations and the corresponding peak densities were 1.0×10^6, 1.1×10^6, and 8.4×10^5 cm^{-3}, respectively. The bottomside density fit is more difficult to achieve at 1900 LT because of the presence of equatorial spread-F. The evening layer is also changing rapidly, and the model results

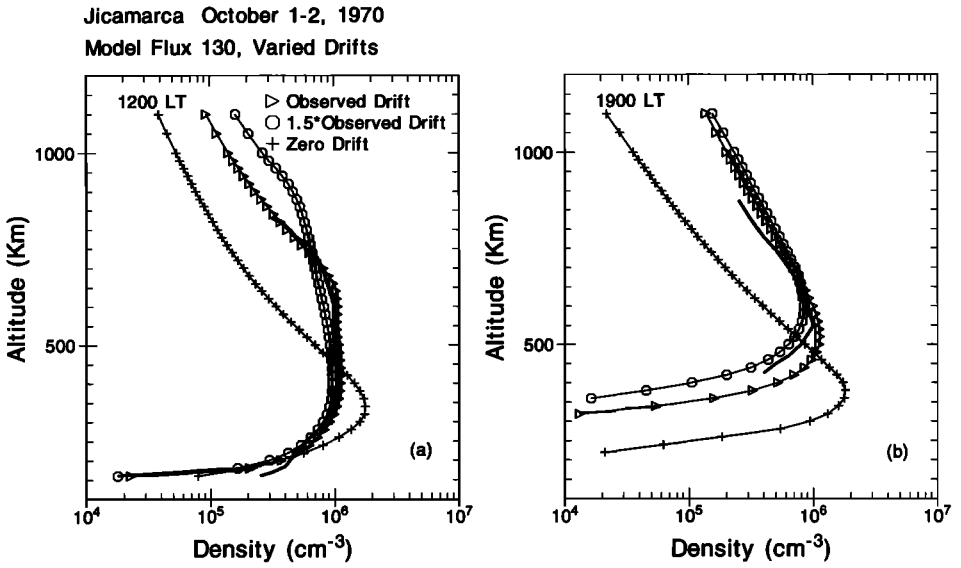

Figure 4. Comparisons of measured and calculated profiles for (a) 1200 and (b) 1900 LT showing the vertical drift effects on the density profiles.

every half hour may not keep up with these changes.

Neutral Wind Effects

We consider now the sensitivity of GTIM to a variety of neutral wind inputs. Both zonal and meridional wind components were used in the model. However, since the declination at Jicamarca is small, the zonal wind effects are not significant, so we did not separate the two components. We used the measured drifts for each case and ran the model assuming zero neutral winds, the standard winds used in the model (HWM-87), and double the standard winds for a 24-hour period. We found that there was no difference in h_mF_2 when the winds were varied, as seen in Figure 5. At night, if the winds were set to zero the peak densities were lower than the measured peaks, if the winds were doubled the peak densities were higher. The main difference occurred in the evening and nighttime topside profiles. During the evening there is little effect on the peak density and layer height, but topside effects are evident. In this case, if the winds are set to zero the topside density is slightly higher than when the winds are included, because less plasma has been transported away from the magnetic equator during the day. In contrast, when the neutral winds are doubled, more ionization is transported away from the magnetic equator during the day and, as expected, the topside ionization is decreased at night. The topside effect is significantly more pronounced later at night.

Our results with respect to the nighttime topside profiles are similar to those reported by *Bailey et al.* [1993]. Our best agreement to the experimental data at night was with calculations where the neutral winds were set to zero, supporting their conclusion that the HWM models may overestimate the nighttime neutral winds in the American sector at equatorial latitudes. It is also possible that improved topside density results require the use of height dependent drift models. Our agreement with the measured h_mF_2 for the 24-hour period is substantially better than Bailey's calculations.

Comparison Between Calculated Results and the IRI90

We also compare our calculations with the most recent version of the IRI model—IRI90. The IRI is a global empirical reference model based on the thirteen standard CCIR-67 parameters obtained from ionosondes, incoherent scatter radars, satellites, and rocket observations or the URSI-89 parameters scaled from ionosondes to provide an average density height profile [*Bilitza*, 1990]. It describes monthly averages of electron density, electron and ion temperatures, and ion composition

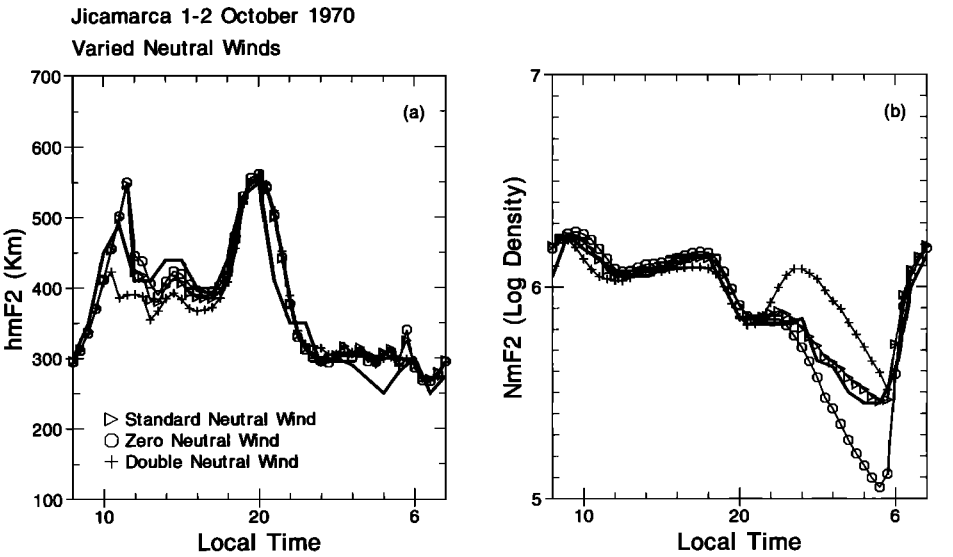

Figure 5. Comparisons of modeled and experimental results when the neutral winds are varied.

from 50 to 1000 km. We ran IRI90 using the URSI-89 coefficients because ionosonde data from Huancayo, Peru, were included in the database [*Rush et al.*, 1984].

The difference between the measured contours and those produced by the IRI90 run with similar solar conditions (not shown here) is striking. There is very little variation in the layer height during the day and little variation in the peak density. There is no indication of the morning and afternoon peaks in N_mF_2, and the effect of the evening prereversal drift enhancement is completely missing. Furthermore, the topside ionosphere is also unrealistic in its rapid decay during the day and high density at night.

In Figure 6 we illustrate peak parameter results with IRI90. The IRI90 peak densities (Figure 6b) compare quite favorably with the data during the early morning hours and during the day. However, around the time of prereversal enhancement the densities from IRI90 are much higher than the measured data because of the lack of prereversal enhancement. There is also no increase in layer height during the day which would lead to the noon bite-out.

In Figure 7 we show an example of the IRI90 profiles to illustrate one of the key problems with modeling the equatorial ionosphere. The IRI90 layer is narrower than the observed data layer, which has consequences when considering total electron content [e.g., *Brown et al.*, 1991]. In fact, the topside of the IRI90 profile at 1200 is almost 300 km lower than the data and the 1900 IRI90 layer is over 100 km lower than the measured data. There is also little change in the profile shape between 1200 and 1900 LT.

Conclusions

We have eliminated one of the input factors to the model by using the observed vertical drifts and have shown that the other assumed inputs such as solar production, loss rates, and neutral atmospheres are realistically described in the model. The agreement between calculated and observed F_2 region peak parameters (h_mF_2 and N_mF_2) and electron density profiles is excellent when the measured vertical drift is used as a model input. An increase in this drift shows the greatest effect on the plasma layer during the evening prereversal enhancement. There is also a good general agreement when the 2-month drift model is used. When the drift is set to zero in the model there is no variation in the plasma layer height and little variation in the density for a 24-hour period. Changes in the neutral wind velocity had no effect on h_mF_2 during equinox, but did alter the nighttime peak densities. A neutral wind velocity input of zero gave better agreement for the topside ionosphere between 2300 and 0400 LT but did not give the best agreement to the peak density

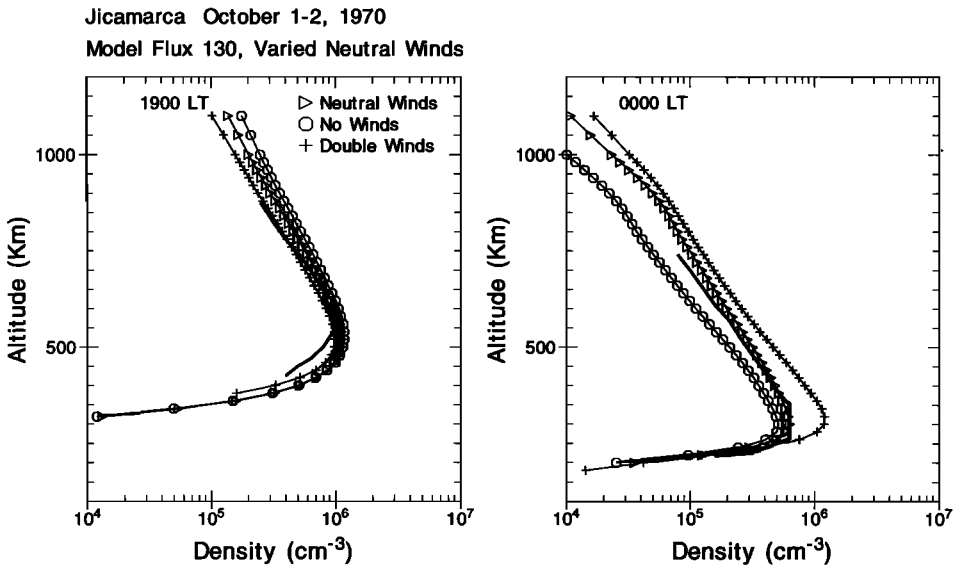

Figure 6. Comparisons of the measured F region peak parameters and IRI90 calculations.

or the peak height at night. The best agreement with the daytime topside ionosphere came when we used the standard neutral wind velocities in GTIM. The theoretical model is highly sensitive to changes in the vertical drift and the neutral winds and these dynamic effects cannot be ignored in modeling the temporal variations of the ionosphere. The climatological approach given by IRI90 is good for describing monthly average values of h_mF_2 and N_mF_2 in the midlatitude region, but the model does not give a good depiction of the low-latitude and equatorial ionospheric regions. This is especially true regarding profile shapes and relates to the problem of a sparse database in the development of the IRI.

Work has been done recently to develop a global vertical drift model using Atmospheric Explorer E satellite data. We will use these drifts to model the equatorial ionosphere at different longitudes.

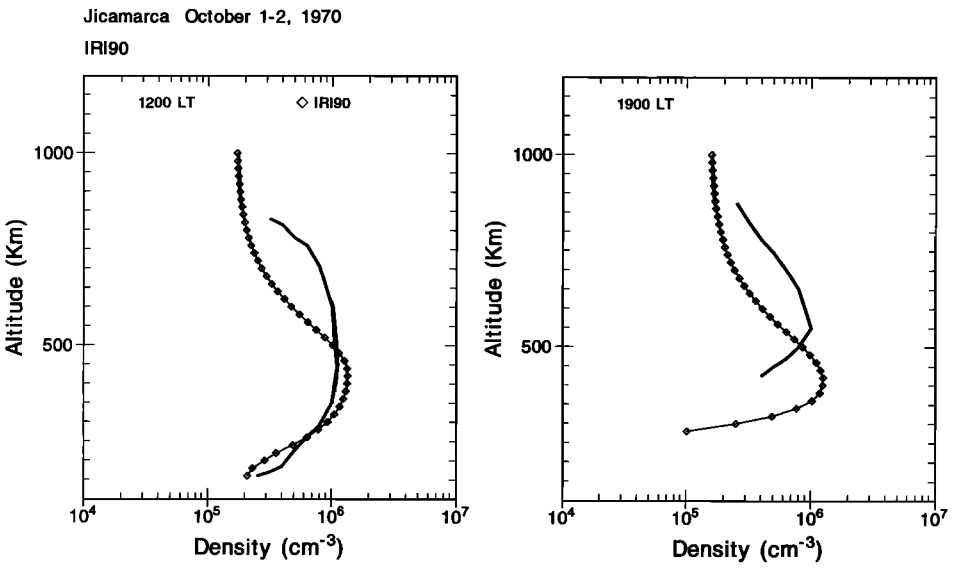

Figure 7. Comparison of the measured profiles and the IRI90 profiles for (a) 1200 and (b) 1900 LT.

Acknowledgments. The authors wish to thank R. Woodman for the Jicamarca measurements and D. B. Zhang for help with the drift data. The work at Utah State was supported by the Aeronomy Program of the National Science Foundation through grant ATM-9102263. The Boston College work is supported by Air Force Contract F19628-90-K-007. The Jicamarca Observatory is operated by the Instituto Geofisico del Peru with support from the National Science Foundation.

References

Anderson, D. N., A theoretical study of the ionospheric *F*-region equatorial anomaly, I, Theory, *Planet. Space Sci.*, *21*, 409–419, 1973a.

Anderson, D. N., A theoretical study of the ionospheric *F*-region equatorial anomaly, II, Results in the American and Asian sectors, *Planet. Space Sci.*, *21*, 421–442, 1973b.

Anderson, D. N., M. Mendillo, and B. Herniter, A semi-empirical low-latitude ionospheric model, *Radio Sci.*, *22*, 292–306, 1987.

Bailey, G. J., R. Sellek, and Y. Rippeth, A modelling study of the equatorial topside ionosphere, *Ann. Geophys.*, *11*, 263–272, 1993.

Bilitza, D., Comparison of measured and predicted F_2 peak altitude, *Adv. Space Res.*, *5*, 29–32, 1985.

Bilitza, D., International Reference Ionosphere 1990, *NSSDC/WDC-A-R & S 90-22*, Goddard Space Flight Center, Greenbelt, Md., Natl. Space Sci. Data Cent., 1990.

Brown, L. D., R. E. Daniell Jr., M. W. Fox, J. A. Klobuchar, and P. H. Doherty, Evaluation of six ionospheric models as predictors of total electron content, *Radio Sci.*, *26*, 1007–1015, 1991.

Chiu, Y. T., An improved phenomenological model of ionospheric density, *J. Atmos. Terr. Phys.*, *37*, 1563–1570, 1975.

Crain, D. J., R. A. Heelis, and G. J. Bailey, Effects of electrical coupling on equatorial ionospheric plasma motions: When is the *F* region a dominant driver in the low-latitude dynamo?, *J. Geophys. Res.*, *98*, 6033–6037, 1993a.

Crain, D. J., R. A. Heelis, and G. J. Bailey, Low-latitude plasma drifts from a simulation of the global atmospheric dynamo, *J. Geophys. Res.*, *98*, 6039–6046, 1993b.

Farley, D. T., Early incoherent scatter observations at Jicamarca, *J. Atmos. Terr. Phys.*, *53*, 665–675, 1991.

Fejer, B. G., Low latitude electrodynamic plasma drifts: A review, *J. Atmos. Terr. Phys.*, *53*, 677–693, 1991.

Fejer, B. G., E. R. de Paula, S. A. Gonzalez, and R. F. Woodman, Average vertical and zonal *F* region plasma drifts over Jicamarca, *J. Geophys. Res.*, *96*, 13,901–13,906, 1991.

Hanson, W. B., and R. J. Moffett, Ionization transport effects in the equatorial *F* region, *J. Geophys. Res.*, *71*, 5559–5572, 1966.

Hedin, A. E., MSIS-86 thermospheric model, *J. Geophys. Res.*, *92*, 4649–4662, 1987.

Hedin, A. E., N. W. Spencer, and T. L. Killeen, Empirical global model of upper thermosphere winds based on Atmospheric and Dynamics Explorer satellite data, *J. Geophys. Res.*, *93*, 9959–9978, 1988.

Hedin, A. E., et al., Revised global model of thermosphere winds using satellite and ground-based observations, *J. Geophys. Res.*, *96*, 7657–7688, 1991.

Hinteregger, H. E., K. Fukui, and B. R. Gibson, Observational, reference, and model data on solar EUV, from measurements on AE-E, *Geophys. Res. Lett.*, *8*, 1147–1150, 1981.

Kelley, M. C., *The Earth's Ionosphere Plasma Physics and Electrodynamics*, 487 pp., Academic, San Diego, Calif., 1989.

Klobuchar, J. A., D. N. Anderson, and P. H. Doherty, Model studies of the latitudinal extent of the equatorial anomaly during equinoctial conditions, *Radio Sci.*, *26*, 1025–1047, 1991.

McClure, J. P., D. T. Farley, and R. Cohen, Ionospheric electron concentration measurements at the magnetic equator, 1964, *ESSA Tech. Rep. ERL 186-AL4*, Natl. Oceanogr. and Atmos. Admin., Boulder, Colo., 1970.

Moffett, R. J., The equatorial anomaly in the electron distribution of the terrestrial *F*-region, *Fundam. Cosmic Phys.*, *4*, 331–391, 1979.

Rush, C. M., M. PoKempner, D. N. Anderson, J. Perry, F. G. Stewart, and R. Reasoner, Global maps of f_oF_2 derived from observational and theoretical values, *Rep. 84-140*, Natl. Telecommun. and Inf. Admin., U.S. Dep. Commer., Washington, D. C., 1984.

Stening, R. J., A two-layer ionospheric dynamo calculation, *J. Geophys. Res.*, *86*, 3543–3550, 1981.

Stening, R. J., Review paper—Modelling the low latitude *F* region, *J. Atmos. Terr. Phys.*, *54*, 1387–1412, 1992.

Sterling, D. L., W. B. Hanson, R. J. Moffett, and R. G. Baxter, Influence of electrodynamic drifts and neutral air winds on some features of the F_2 region, *Radio Sci.*, *4*, 1005–1023, 1969.

Sterling, D. L., W. B. Hanson, and R. F. Woodman, Synthesis of data obtained at Jicamarca, Peru, during the September 11, 1969, eclipse, *Radio Sci.*, *7*, 279–289, 1972.

Strobel, D. F., and M. B. McElroy, The F_2-layer at middle latitudes, *Planet. Space Sci.*, *18*, 1181–1202, 1970.

Woodman, R. F., and T. Hagfors, Methods for the measurement of vertical ionospheric motions near the magnetic equator by incoherent scattering, *J. Geophys. Res.*, *74*, 1205–1212, 1969.

Woodman, R. F., D. L. Sterling, and W. B. Hanson, Synthesis of Jicamarca data during the great storm of March 8, 1970, *Radio Sci.*, *7*, 739–746, 1972.

D. N. Anderson, Ionospheric Effects Branch, PL/GPIM, 29 Randolph Road, Hanscom Air Force Base, MA 01731. (e-mail: danderson@plh.af.mil)

P. H. Doherty, Institute for Space Research, Boston College, Newton, MA 02159. (e-mail: doherty@phl.af.mil)

B. G. Fejer, Center for Atmospheric Space Sciences, Utah State University, Logan, UT 84322. (e-mail: usu::bfejer)

A. J. Preble, Flight Test Branch, Phillips Laboratory, PL/WE, 3550 Aberdeen Ave., S. E., Kirtland Air Force Base, NM 87117. (e-mail: preble@plh.af.mil)

(Received September 13, 1993; revised March 4, 1994; accepted March 10, 1994.)